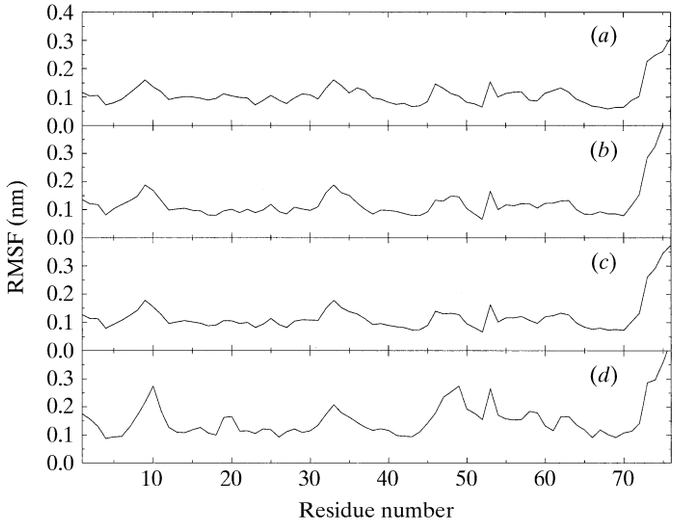

Fig. 20.1.3.7. Root-mean-square Cα-atom-position fluctuations (RMSFs) in nm are shown using the same averaging periods as in Fig. 20.1.3.6, but averaged over all four protein molecules in the unit cell.

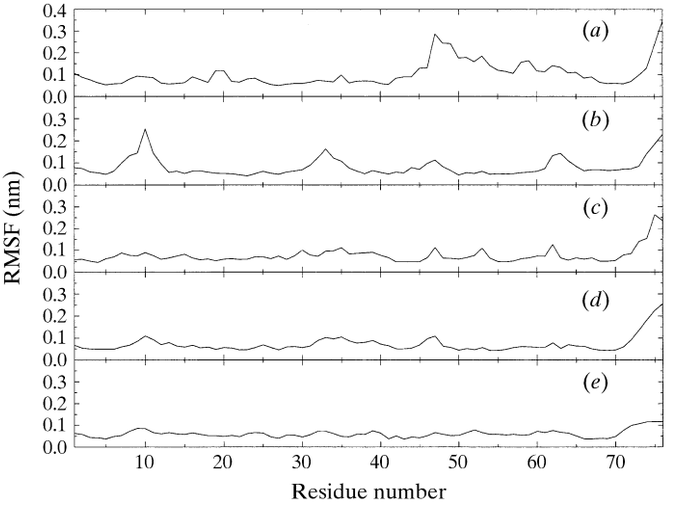

Fig. 20.1.3.8. Root-mean-square Cα-atom-position fluctuations (RMSFs) in nm for the four protein molecules in the unit cell as a function of the residue number. Full translational and rotational fitting was applied to the Cα atoms of residues 1–72 using the final 1.6 ns of the simulation [(*a*)–(*d*)]. (*e*) shows the corresponding values defined by equation (20.1.3.1), obtained from experimental *B* factors.

another indication that the single-chain movements are converged on these short timescales. In the last 800 ps of the simulation, the RMSFs are substantially higher than in the 800 ps window before that. All of the peaks can be traced back to one of the single chains. If only one of the four molecules differs strongly from the other three, this one determines the magnitude of the fluctuations of the average. The peak at residue 10 comes from chain 2, the ones around residue 20 and the whole region 47–64 are determined by chain 1. The peak at residue 33 originates in chain 3, which at this point differs substantially from the mean MD structure (Fig. 20.1.3.3).

20.1.3.5. *Internal motions of the proteins*

Fig. 20.1.3.8 displays the atomic root-mean-square position fluctuations for the Cα atoms of the four protein molecules during the whole analysis period, together with corresponding values obtained using equation (20.1.3.1) and the crystallographic *B* factors. Rotational and translational fitting was applied using the Cα atoms of residues 1–72, and the fluctuations were averaged over the final 1.6 ns. The mobility of the stable secondary-structure elements in the simulation is comparable with that inferred from the experiment. There is a correlation between the more mobile parts of the proteins in the simulation and large *B* factors in the X-ray structure, but the magnitude of the fluctuations is overestimated in the simulation. The movements of the single chains can be rationalized as follows. In chain 1, the whole region from Gly47 onwards rotates around a stable axis formed by residues 41–46. This part lies, as do all the flexible regions, on the exterior of the protein. Residues 19 and 20, which are stable in all but this single chain, are in contact with this moving part. This rotation, which tends to compact the protein, occurs during the 200 ps period between 1350 and 1550 ps after the start of the simulation, in which the atom-position RMSD from the X-ray structure increases significantly (Fig. 20.1.3.2). Overall, chain 2 is more stable than chain 1. Nevertheless, the end of the unwinding helix shows large fluctuations. In the course of this deformation, the side-chain nitrogen atom of Lys11 moves from close to the OE atom of Glu34 towards the backbone oxygen atom of Lys33, which is associated with a change in the position of Gly10. A similar but smaller motion occurs in chain 4. Both lysines, Lys33 and Lys63, are fully exposed to the solvent and have no intramolecular contacts. In chain 3, the flexible residues are also not part of secondary-structure elements and are located on the outside of the protein. The backbone oxygen atom of Gln62 that moves in all the four chains has, in addition, the closest contact to another heavy atom: the OG1 atom of Ser65 is only 2.51 Å away, and the van der Waals repulsion of these atoms causes them to move further away from one another. The mobile residues in chain 4 are again in contact with the solvent, Gly35, Gly47, Gln62, the end of the helix and Gly10. The terminal residues of all the protein molecules are very mobile, as observed experimentally in the crystal.

20.1.3.6. *Dihedral-angle fluctuations and transitions*

Backbone dihedral-angle fluctuations and transitions are examined in Tables 20.1.3.3 and 20.1.3.4 using different analysis periods. After the first 400 ps of analysis, the φ/ψ dihedral-angle fluctuations differ only slightly, but if longer averaging times are chosen, the different protein molecules show larger differences from one another. These fluctuations also increase for longer analysis times, indicating that they are not yet converged after 2 ns. In the period from 800 to 1200 ps, chain 3 shows a large increase in mean-square dihedral-angle fluctuations, whereas the Cα-atom-position RMSDs with respect to the X-ray structure during the same time fluctuate around a plateau. Thus, there is a lot of flexibility without the simulation structure diverging from the experimental one. Protein molecule 3, for example, shows the largest φ/ψ fluctuations of all the four molecules, and it shows the lowest atom-position RMSDs of Cα atoms from the X-ray structure at the end of the simulation (Fig. 20.1.3.2), indicating that it explores phase space around the equilibrium structure. If, in contrast, the Cα-atom-position RMSDs, with respect to the X-ray structure, increase significantly, larger dihedral-angle fluctuations are also observed, for example, in molecule 1 after 1200 ps.

Concerning relaxation, observations similar to those made before can be made when analysing dihedral-angle transitions (Table 20.1.3.4). The number of transitions for the different chains differs by about 20%. Within a single chain, however, the number of transitions increases in proportion to the observation time. Again, the protein molecules showing the most transitions do not have the largest Cα-atom-position RMSDs from the X-ray structure. Thus,

references